

## Synopsis

Different coordination modes of the o-phenylenedioxydiacetato ligand (PDOA) lead to a ribbon-like arrangement of  $\{\text{Ce}_3\}$  triangles in  $[\text{Ce}(\text{PDOA})(\text{NO}_3)(\text{H}_2\text{O})_2]_n$  (**1**) and to zig-zag chains in  $\{[\text{Ce}(\text{PDOA})(\text{NO}_3)(\text{H}_2\text{O})_3] \cdot \text{H}_2\text{O}\}$  (**2**); in both structures *syn-anti* carboxylate bridges link the Ce(III) atoms. A magnetic study using data at temperatures above 50 K reveals Curie-Weiss behavior for **1** with  $\theta = -35.5$  K.

Two novel coordination polymers in the family of lanthanide complexes with o-phenylenedioxydiacetato as ligand

Monika Stolárová<sup>a</sup>, Juraj Černák<sup>a,\*</sup>, Milagros Tomás<sup>b</sup>, Irene Ara<sup>b</sup>, Martin Orendáč<sup>d</sup>, Larry R. Falvello<sup>c,\*</sup>

<sup>a</sup> Department of Inorganic Chemistry, Faculty of Sciences, P. J. Šafárik University in Košice, Moyzesova 11, 041 54 Košice, Slovakia

<sup>b</sup> Departamento de Química Inorgánica, Instituto de Síntesis Química y Catálisis Homogénea (iSQCH), University of Zaragoza-CSIC, Pedro Cerbuna 12, E-50009, Zaragoza, Spain

<sup>c</sup> Departamento de Química Inorgánica, Instituto de Ciencia de Materiales de Aragón(ICMA), University of Zaragoza-CSIC, Pedro Cerbuna 12, E-50009 Zaragoza, Spain

<sup>d</sup> Institute of Physics, P. J. Šafárik University in Košice, Park Angelinum 9, 041 54 Košice, Slovakia

Correspondence email: [juraj.cernak@upjs.sk](mailto:juraj.cernak@upjs.sk), [falvello@unizar.es](mailto:falvello@unizar.es)

## Abstract

Two novel coordination polymers  $[\text{Ce}(\text{PDOA})(\text{NO}_3)(\text{H}_2\text{O})_2]_n$  (**1**) and  $\{[\text{Ce}(\text{PDOA})(\text{NO}_3)(\text{H}_2\text{O})_3] \cdot \text{H}_2\text{O}\}_n$  (**2**) (PDOA = o-phenylenedioxydiacetato) have been prepared using hydrothermal conditions and have been structurally characterized. In both crystal structures **1** and **2** the Ce(III) atoms are decacoordinated by oxygen atoms from PDOA ligands with chelating and bridging functions, chelating nitrate ligands and aqua ligands. While in **1** the PDOA ligand presents a hexadentate coordination mode, in **2** it is coordinated in a pentadentate manner; this difference leads to different types of one-dimensional structural motifs: in **2** there are zig-zag chains of the -Ce-O-C-O-Ce- type with *syn-anti* carboxylate bridges and in **1** these chains are additionally interlinked by further *syn-anti* carboxylate bridges leading to a strip- or ribbon-like arrangement formed of  $\{\text{Ce}_3\}$  fused triangles. The endothermic dehydration of **1** within the temperature range 69-199 °C is at least a two-step process as suggested by TG and DTA methods. A variable temperature (2-300 K) magnetic study reveals Curie-Weiss behavior for **1** with  $\theta = -35.5$  K observed above 50 K. The origin of the observed behavior is discussed.

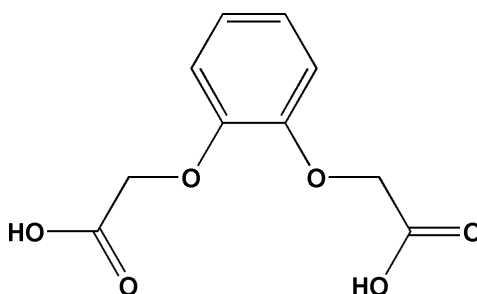
**Keywords:** coordination polymer; Ce(III) complex; crystal structure; nitrate; o-phenylenedioxydiaceto ligand

## 1. Introduction

Increasing interest in the design, synthesis and characterization of new lanthanide complexes has been stimulated by their structural diversity and potential applications in catalysis,

1  
2  
3  
4  
5  
6  
7  
8  
9  
10  
11  
12  
13  
14  
15  
16  
17  
18  
19  
20  
21  
22  
23  
24  
25  
26  
27  
28  
29  
30  
31  
32  
33  
34  
35  
36  
37  
38  
39  
40  
41  
42  
43  
44  
45  
46  
47  
48  
49  
50  
51  
52  
53  
54  
55  
56  
57  
58  
59  
60  
61  
62  
63  
64  
65

fluorescence/light emission, magnetism and as functional materials in the field of MOFs [1-7]. Polycarboxylic acids (and their deprotonized forms) in particular have received a great deal of attention due to their ability to act as chelating as well as bridging ligands in lanthanide complexes with various structural dimensionalities [8-12]. Among the polycarboxylic acids, *o*-phenylenedioxydiacetic acid, H<sub>2</sub>PDOA (Scheme 1) exhibits, after deprotonation, various multidentate chelating and/or bridging modes of coordination with lanthanide ions [13-16].



<Scheme 1> Structure of H<sub>2</sub>PDOA

Up to now, according to a search in CSD [17], only one compound containing Ce(III) and the PDOA ligand has been structurally characterized, namely {[Ce<sub>2</sub>(PDOA)<sub>3</sub>(H<sub>2</sub>O)<sub>6</sub>]·2H<sub>2</sub>O}<sub>n</sub>, [18,19]. Herein, as a part of our broader study on lanthanide complexes with PDOA, we report the syntheses, properties and crystal structures of two novel Ce(III) complexes, [Ce(PDOA)(NO<sub>3</sub>)(H<sub>2</sub>O)<sub>2</sub>]<sub>n</sub> (**1**) and {[Ce(PDOA)(NO<sub>3</sub>)(H<sub>2</sub>O)<sub>3</sub>]·H<sub>2</sub>O}<sub>n</sub> (**2**) along with the magnetic properties of **1**.

## 2. Experimental

### 2.1. General considerations

CHN analyses were performed on a Perkin Elmer 2400 Series II CHNS/O analyzer. Infrared spectra were recorded on a Perkin Elmer Spectrum 100 CsI DTGS FTIR Spectrometer with UATR 1 bounce-KRS-5 in the range of 4000–300 cm<sup>-1</sup>. X-ray powder patterns were measured on a RIGAKU D-Max/2500 diffractometer with rotating anode and RINT2000 vertical goniometer, in the range 3-60° of 2θ using Cu Kα<sub>1,2</sub> radiation (λ = 1.5406 Å). The calculated patterns were obtained using the program Mercury CSD 3.1.1 Development [20]. TG and DTG curves were recorded on a 2960 SDT V3.0 F instrument (aluminum crucibles) in a nitrogen atmosphere in the temperature range 20-250 °C with heating rate 5°/min.

### 2.2. Magnetic measurements

The magnetic properties of **1** were investigated using a commercial Quantum Design SQUID magnetometer in the temperature range from 2 to 300 K at 0.1 T. The powder specimen (86.5 mg) was fixed in a gelcap using varnish GE 7031 and the gelcap was held by a straw. The signal contribution of the varnish, empty gelcap and the straw was subtracted from the

total signal. The obtained data were corrected the diamagnetic contribution using Pascal's constants [21].

### 2.3. X-ray crystallography

Single-crystal X-ray data were collected at 100(1) K on a Bruker CCD-based three-circle diffractometer equipped with a graphite monochromator utilizing MoK $\alpha$  radiation ( $\lambda = 0.71073 \text{ \AA}$ ). Absorption corrections were based on the multi-scan technique using SADABS [22]. The structures were solved by SIR92 [23] and refined against the  $F^2$  data using full-matrix least squares methods with the program SHELXL-97 [24]. Anisotropic displacement parameters were refined for all non-H atoms. The hydrogen atoms bonded to carbon and oxygen atoms were included at idealized positions and refined as riders with isotropic displacement parameters assigned as 1.2 times the  $U_{eq}$  values of the corresponding bonding partners. The crystal and experimental data are given in Table 1, and selected geometric parameters are given in Table 2. Possible hydrogen bonds are gathered in Tables 3 and 4. The structural figures were drawn using Diamond [25].

### 2.4 Syntheses of $[\text{Ce}(\text{PDOA})(\text{NO}_3)(\text{H}_2\text{O})_2]_n$ (**1**) and $\{[\text{Ce}(\text{PDOA})(\text{NO}_3)(\text{H}_2\text{O})_3] \cdot \text{H}_2\text{O}\}_n$ (**2**)

A mixture of 0.087 g of  $\text{Ce}(\text{NO}_3)_3 \cdot 6\text{H}_2\text{O}$  (0.2 mmol), 0.068 g of  $\text{H}_2\text{PDOA}$  (0.3 mmol) and 0.04 g of 1,10-phenanthroline monohydrate (0.2 mmol) with 10  $\text{cm}^3$  of water was placed in a 25  $\text{cm}^3$  glass flask, heated in the oven at 393 K for 48 hours and then cooled to room temperature at a rate of 8 deg/h. The resulting colorless solution was filtered and layered with 10  $\text{cm}^3$  of 2-propanol. A mixture of crystals of **1** and **2** was formed within four days at the interface of the two phases.

Compound **1** was also prepared using the following procedure: a mixture of 0.217 g of  $\text{Ce}(\text{NO}_3)_3 \cdot 6\text{H}_2\text{O}$  (0.5 mmol), 0.113 g of  $\text{H}_2\text{PDOA}$  (0.5 mmol) with 1  $\text{cm}^3$  of aqueous solution of 1M NaOH in water was placed in a 25  $\text{cm}^3$  glass flask, which was heated in the oven at 398 K for 48 h and then cooled to room temperature at a rate of 7 deg/h. The resulting colorless solution was filtered and within a few days small crystals of **1** separated. Yield: 40 %

Anal. CHNS/O of **1**:  $\text{C}_{10}\text{H}_{12}\text{Ce}_1\text{N}_1\text{O}_{11}$  ( $M = 462.33 \text{ g}\cdot\text{mol}^{-1}$ ): Found (%): C, 25.97; H, 2.58; N, 3.08; Calc. (%): C, 25.98; H, 2.62; N, 3.03.

IR (UATR) of **1** (in  $\text{cm}^{-1}$ ): 3478(w); 3159(w); 3085(w); 2918(w); 1603(s); 1501(s); 1457(m); 1424(s); 1331(s); 1288(m); 1247(s); 11921(m); 1119(s); 1031(m); 951(w); 819(m); 759(m); 690(m); 596(s); 571(s); 520(s); 437(m); 342(m).

IR (UATR) of **2** (in  $\text{cm}^{-1}$ ): 3212(m); 3091(w); 2936(w); 1692(w); 1593(s); 1501(s); 1478(m); 1451(m); 1421(s); 1344(m); 1303(m); 1247(s); 1195(m); 1124(s); 1032(m); 959(m); 921(w); 817(m); 765(m); 750(m); 716(m); 693(s); 603(s); 582(s); 525(s); 461(m); 431(m); 327(m).

<Table 1> Crystal data and structure refinements for **1** and **2**

	<b>1</b>	<b>2</b>
Empirical formula	C <sub>10</sub> H <sub>12</sub> Ce N O <sub>11</sub>	C <sub>10</sub> H <sub>16</sub> Ce N O <sub>13</sub>
Molecular weight	462.33	498.36
Crystal system	monoclinic	monoclinic
Space group	P2 <sub>1</sub> /c	P2 <sub>1</sub> /c
Unit cell dimensions		
<i>a</i> (Å)	15.440(1)	14.632(1)
<i>b</i> (Å)	6.1429(3)	12.186(1)
<i>c</i> (Å)	16.790(1)	9.0427(6)
$\beta$ (°)	115.600(1)	100.413(1)
<i>V</i> (Å <sup>3</sup> )	1436.1(5)	1585.8(5)
<i>Z</i>	4	4
<i>D</i> <sub>calc</sub> (Mg.m <sup>-3</sup> )	2.138	2.087
<i>T</i> (K)	100(2)	100(2)
$\mu$ (mm <sup>-1</sup> )	3.231	2.943
Crystal dimensions (mm)	0.12x0.11x0.03	0.22 x 0.06 x 0.04
Crystal color / form	beige plate	colorless needle
Index ranges	-20 ≤ <i>h</i> ≤ 13 -8 ≤ <i>k</i> ≤ 7 -20 ≤ <i>l</i> ≤ 22	-18 ≤ <i>h</i> ≤ 17 -14 ≤ <i>k</i> ≤ 15 -11 ≤ <i>l</i> ≤ 8
$\theta$ ranges (°)	1.46 – 28.61	1.42 – 26.19
Reflections collected	3369	3168
Independent reflections	3160 ( <i>R</i> <sub>int</sub> = 0.0252)	2806 ( <i>R</i> <sub>int</sub> = 0.0323)
Absorption corr. method	multi-scan	multi-scan
<i>T</i> <sub>min</sub> <i>T</i> <sub>max</sub>	0.6131-0.7457	0.6257-0.7453
Goodness-of-fit on <i>F</i> <sup>2</sup>	1.062	1.188
<i>R</i> indices [ <i>I</i> > 2σ( <i>I</i> )]	<i>R</i> <sub>1</sub> = 0.0210, <i>wR</i> <sub>2</sub> = 0.0502	<i>R</i> <sub>1</sub> = 0.0251, <i>wR</i> <sub>2</sub> = 0.0593
<i>R</i> indices (all data)	<i>R</i> <sub>1</sub> = 0.0229, <i>wR</i> <sub>2</sub> = 0.0514	<i>R</i> <sub>1</sub> = 0.0317, <i>wR</i> <sub>2</sub> = 0.0804
Diff. peak and hole (e.Å <sup>-3</sup> )	1.200; -0.754	0.821; -0.465

### 3. Results and Discussion

#### 3.1 Preparation and identification of [Ce(PDOA)(NO<sub>3</sub>)(H<sub>2</sub>O)<sub>2</sub>]<sub>n</sub> (**1**) and {[Ce(PDOA)(NO<sub>3</sub>)(H<sub>2</sub>O)<sub>3</sub>·H<sub>2</sub>O]<sub>n</sub> (**2**)

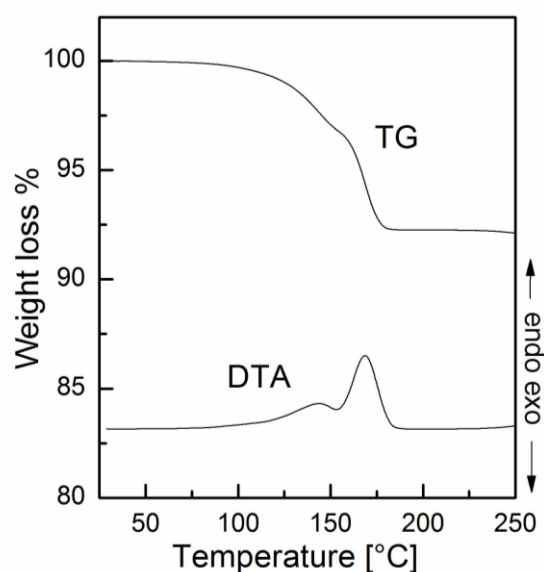
Complex **1** was prepared by two different procedures using hydrothermal conditions, in one case by a targeted synthesis and in the other by a procedure that was not originally intended to give this product. In the presence of phen, a mixture of crystals of complexes **1** and **2** is

1  
2  
3  
4  
5  
6  
7  
8  
9  
10  
11  
12  
13  
14  
15  
16  
17  
18  
19  
20  
21  
22  
23  
24  
25  
26  
27  
28  
29  
30  
31  
32  
33  
34  
35  
36  
37  
38  
39  
40  
41  
42  
43  
44  
45  
46  
47  
48  
49  
50  
51  
52  
53  
54  
55  
56  
57  
58  
59  
60  
61  
62  
63  
64  
65

obtained; these crystals, suitable for X-ray data collection, were separated manually under a microscope and further studied. We note that our effort to prepare single crystals using the same procedure, but in the absence of phen, was not successful. As complex **2** was formed only as an admixture, it was only partially characterized, while a fuller characterization including a magnetic study is given for **1** (see below). The phase purity and identity of **1** was checked by comparison of the experimental X-ray powder diffraction pattern with the one calculated on the basis of the known crystal structure (see Fig. S1 in the Supplementary material).

IR spectra of both **1** and **2** were recorded. The positions of the observed absorption bands are gathered in the experimental part for identification purposes. The IR spectra are rich especially due to the presence of the PDOA ligands in the complexes, so the unambiguous assignment of the observed absorption bands is difficult. Nevertheless, bands arising from asymmetric and symmetric  $\nu(\text{COO})$  vibrations of the carboxylates are characteristic of **1** and **2**, the asymmetric  $\nu(\text{COO})$  vibrations are observed at 1603 (**1**) and 1593 (**2**)  $\text{cm}^{-1}$ , while the absorption bands at 1332  $\text{cm}^{-1}$  for **1**, and at 1344  $\text{cm}^{-1}$  for **2** are assigned to the symmetric  $\nu(\text{COO})$  vibrations. Usual values for  $\nu_{\text{as}}(\text{COO}^-)$  are in the range of 1610-1550  $\text{cm}^{-1}$  for the asymmetric modes and 1400-1300  $\text{cm}^{-1}$  for symmetric  $\nu(\text{COO}^-)$  [26]. All assigned values correspond to those in the previously reported compound  $\text{Na}[\text{Yb}(\text{PDOA})_2(\text{H}_2\text{O})_2]\cdot 2\text{H}_2\text{O}$  [27].

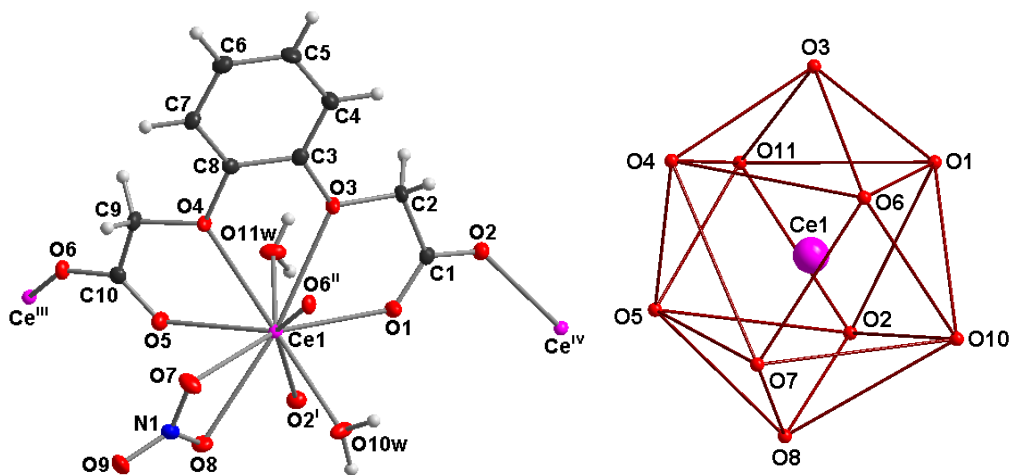
In order to estimate the water contents and to follow the dehydration process in **1** its TG and DTA curves up to 250 °C were recorded. The dehydration process of **1** is observed in the temperature range 69-199 °C and the observed weight loss is 7.7 %. This value corresponds well to the calculated value of 7.8 % for full dehydration. As indicated by the DTA curve the dehydrations of **1** is at least a two-step endothermic process (Fig. 1).



<Fig. 1> TG and DTA curves for **1**.

### 3.2 Crystal structures

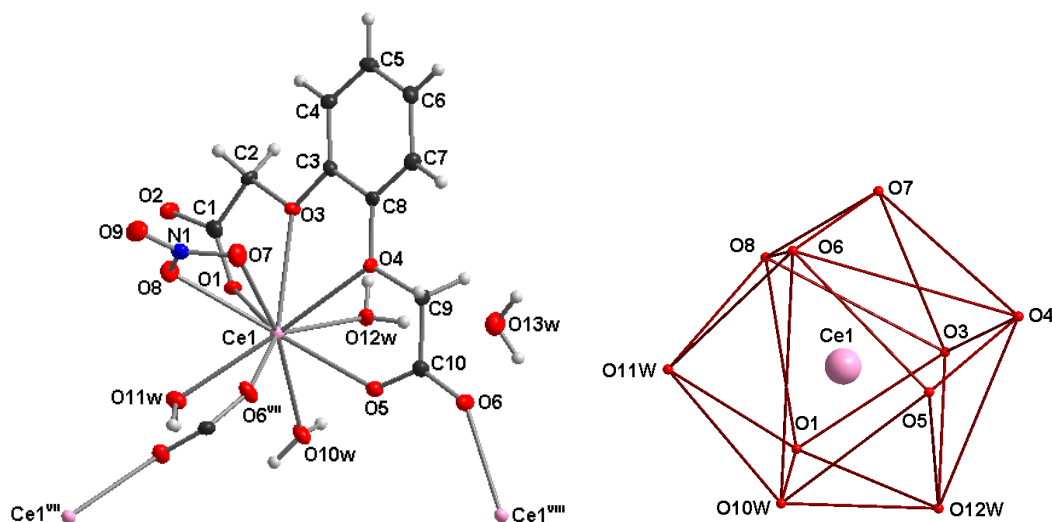
The central Ce(III) atoms in both **1** and **2** exhibit deca-coordination (Fig. 2, Fig. 3). In **1** the O<sub>10</sub> donor set is formed by four oxygen atoms (O1, O3, O4, O5) originating from the chelating function of the hexadentate PDOA ligand, two oxygen atoms (O2 and O6) from two further, crystallographically different, PDOA ligands, and by a further four oxygen atoms, two from a chelating nitrate ligand (O7 and O8) and two (O10w and O11w) from aqua ligands (Fig 2). Using the program SHAPE [28] the resulting coordination polyhedron was identified as a bicapped square antiprism.



<Fig. 2> The coordination mode of the Ce(III) atom in **1** (left) and the view of the coordination polyhedron (right). Symmetry codes: i: 1-x, 1/2+y, 1/2-z; ii: x, y-1, z; iii: x, 1+y, z; iv: 1-x, y-1/2, 1/2-z

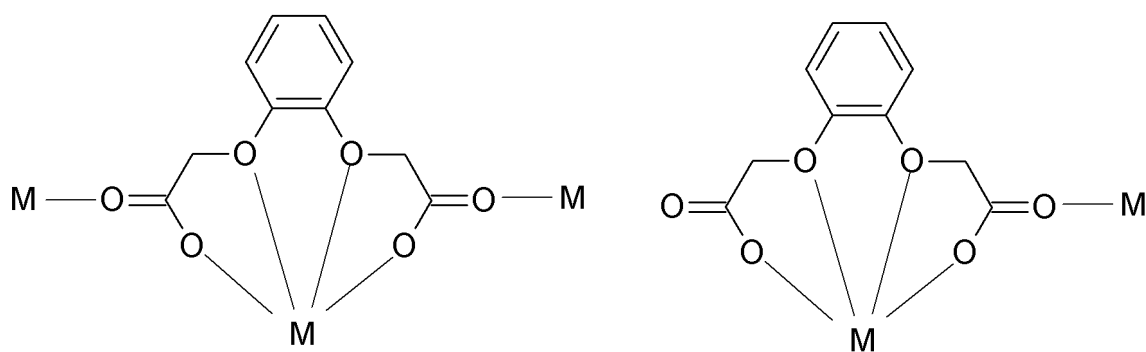
The O<sub>10</sub> donor set for the Ce(III) atom in **2** is composed of four oxygen atoms (O1, O3, O4, O6) originating from the chelating pentadentate PDOA ligand, one oxygen atom from a symmetry related PDOA ligand (O6<sup>ii</sup>; ii: x, y-1, z) that links two Ce(III) atoms through a carboxylate bridge, two oxygen atoms from the chelating nitrate ligand (O7 and O8) and three aqua ligands (O10w, O11w and O12w) (Fig. 3). The coordination polyhedron around the Ce(III) atoms, rather irregular as a result of the disposition of the chelating nitrate ligand, was identified using the program SHAPE [28] to be best described as a sphenocorona.





<Fig. 3> The coordination around the Ce(III) atom in **2** (left) and the resulting polyhedron (right). Symmetry codes: vii: x, 5/2-y, z-1/2; viii: x, 5/2-y, z+1/2

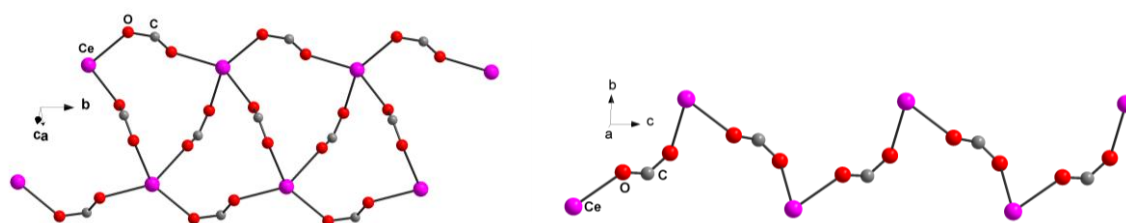
The different chelating-bridging coordination modes of the PDOA ligands in **1** and **2** are schematically depicted in Scheme 2. As can be seen, in **1** the PDOA ligand is hexadentate: it uses four “inner” oxygen atoms for chelation while the two “outer” carboxyl oxygen atoms coordinate to a further two crystallographically independent Ce(III) atoms forming bridges (Scheme 2-left). This coordination mode is not common but it was observed, *e.g.*, in  $[\text{Na}_2\text{Ca}(\text{PDOA})_2(\text{H}_2\text{O})_5] \cdot 2\text{H}_2\text{O}$  [29]. In contrast, in **2** the PDOA ligand is pentadentate as only one “outer” carboxyl oxygen atom is used for coordination to an additional Ce(III) atom (Scheme 2-right). The same coordination mode was already observed in  $[\text{Ln}(\text{PDOA})_3(\text{H}_2\text{O})_6] \cdot 2\text{H}_2\text{O}$  (Ln = Eu, Dy, Sm) [14].



<Scheme 2> The coordination modes of PDOA ligand in **1** (left) and **2** (right).

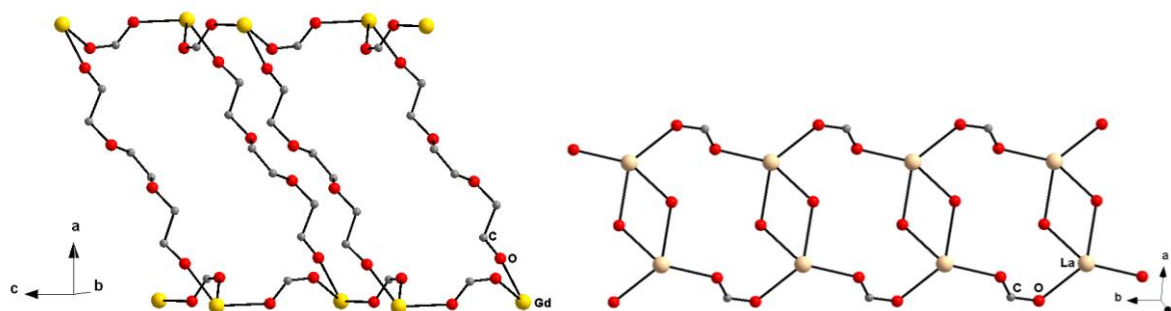
Both **1** and **2** exhibit topologically different one-dimensional (1d) crystal structures which can be regarded as a consequence of the different bridging modes of the PDOA ligands (Fig. 4); we note that the nitrate ligands act only as blocking ligands. In **1** each Ce(III) atom is linked

1 to four neighbouring Ce(III) centres by four *syn-anti* carboxylate bridges  $[-O-C-O-]$   
 2 (connectivity of the node formed by Ce(III) is four) forming a 1d ribbon structure running  
 3 along the *b* axis; alternatively, the ribbon or strip can be described as built up of fused  
 4 triangles  $\{Ce_3\}$  with Ce(III) atoms at the vertices (Fig. 4). On the other hand, in the crystal  
 5 structure of **2** each Ce(III) atom is connected with only two other Ce(III) atoms *via syn-anti*  
 6 carboxylate bridges (connectivity two) which leads to the formation of zig-zag chains running  
 7 along *c* axis. A search in the CSD [17] revealed that, up to now, for *o*-  
 8 phenylenedioxydiacetato lanthanide complexes only two ladder-like structural motifs were  
 9 reported, one with long rungs and one with short rungs (Fig. 5). All but one of the long-rung  
 10 systems are isostructural. As an example of the isostructural series we can mention  
 11  $[Gd_2(PDOA)_3(H_2O)_6] \cdot 2H_2O$  (Fig. 5, left) [19]. On the other hand, the second ladder-like  
 12 structural motif with short legs formed by a pair of  $\mu_2$ -oxo bridges was observed  
 13  
 14  
 15  
 16  
 17  
 18  
 19  
 20  
 21  
 22  
 23  
 24  
 25  
 26  
 27  
 28  
 29  
 30  
 31  
 32  
 33  
 34  
 35



36  
 37  
 38  
 39  
 40  
 41  
 42  
 43  
 44  
 45  
 46  
 47  
 48  
 49  
 50  
 51  
 52  
 53  
 54  
 55  
 56  
 57  
 58  
 59  
 60  
 61  
 62  
 63  
 64  
 65

<Fig. 4> The ribbons in **1** (left) and zig-zag chains in **2** (right). Only atoms participating in propagation of the structures are shown.



<Fig. 5> The formed ladders in  $[Gd_2(PDOA)_3(H_2O)_6] \cdot 2H_2O$  (left) [19] and in  $[La(PDOA)Cl(H_2O)_2]$  (right) [30]. Only atoms participating in propagation of the structure are shown.

<Table 2> Selected geometric parameters [ $\text{\AA}$ ,  $^\circ$ ] for **1** and **2**.

<b>1</b>		<b>2</b>	
Ce1-O1	2.4417(16)	Ce1-O1	2.474(3)
Ce1-O2 <sup>i</sup>	2.5205(16)	Ce1-O3	2.647(3)
Ce1-O3	2.7905 (16)	Ce1-O4	2.685(3)
Ce1-O4	2.6640 (16)	Ce1-O5	2.468(3)
Ce1-O5	2.4691(17)	Ce1-O6 <sup>vii</sup>	2.473(3)
Ce1-O6 <sup>ii</sup>	2.4997(16)	Ce1-O7	2.736(3)
Ce1-O7	2.6079(17)	Ce1-O8	2.628(3)
Ce1-O8	2.6852(16)	Ce1-O10w	2.560(3)
Ce1-O10w	2.5158(18)	Ce1-O11w	2.576(3)
Ce1-O11w	2.5111(18)	Ce1-O12w	2.531(3)
O7-N1	1.262(3)	O7-N1	1.261(5)
O8-N1	1.262(2)	O8-N1	1.288(5)
O9-N1	1.237(2)	O9-N1	1.220(5)

Symmetry codes: i: 1-x, 1/2+y, 1/2-z; ii: x, y-1, z; vii: x, 5/2-y, z-1/2

only in  $[\text{La}(\text{PDOA})\text{Cl}(\text{H}_2\text{O})_2]$  (Fig. 6, right) [30]. Nevertheless, in both structural types, in contrast to **1** and **2**, the lanthanide atoms are linked by covalent bridges to three neighbouring lanthanide atoms (connectivity three) [19,30]. Thus, the observed 1d structural motifs in **1** and **2** represent novel types within the structural chemistry of lanthanides with o-phenylenedioxydiacetato ligand.

The Ce-O bond distances in **1** and **2** are in the ranges of 2.442(2) – 2.791(2)  $\text{\AA}$  and 2.468(3) – 2.736(3)  $\text{\AA}$ , respectively. The longest Ce-O bonds are formed by phenolato and nitrate oxygen atoms, suggesting their weaker coordination (Table 2). Similar ranges of Ce-O bonds were observed in  $\{[\text{Ce}_2(\text{PDOA})_3(\text{H}_2\text{O})_6]\cdot 2\text{H}_2\text{O}\}_n$  (range 2.3802(17) - 2.7032(14)  $\text{\AA}$ ) [19] and  $\{[\text{Ce}(\text{HPAA})_2(\text{NO}_3)(\text{H}_2\text{O})_2]\cdot \text{H}_2\text{O}\}_n$  (range 2.4914(14) - 2.7245(15)  $\text{\AA}$ ; HPAA = 2-(4-hydroxyphenyl)acetate) [31].

Both crystal structures, **1** and **2**, are further stabilized by hydrogen bonding interactions. As can be seen from Fig. 6, all water molecules along with the two nitrate oxygen atoms (O8 and O9) and two oxygen atoms from PDOA ligands (O1 and O5) are involved in medium-strength hydrogen bonds (HBs) of the O-H...O type with D...A distances in the range 2.625(3) - 2.868(3)  $\text{\AA}$  (Table 2, Fig. 6). Two of the HBs are intramolecular (*i.e.*, they link atoms within the ribbons), while a further two HBs, involving nitrate oxygen atoms, are intermolecular and link neighboring strips. As a consequence, a ring system of HBs with descriptor  $R_2^2(8)$  involving two Ce(III) atoms can be distinguished. This ring can be seen at the centre of Fig. 6.

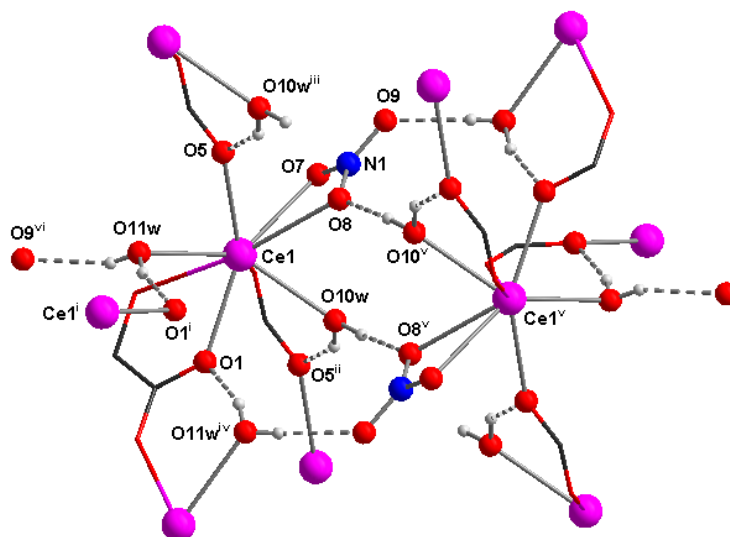


Fig. 6 Hydrogen bonding system in **1**. Some atoms not participating in HBs formation are shown only as wires. Symmetry codes: i: 1-x, 1/2+y, 1/2-z; ii: x, y-1, z; iii: x, 1+y, z; iv: 1-x, y-1/2, 1/2-z; v: 1-x, -y, -z; vi: x, 1/2-y, 1/2+z.

The hydrogen bonding system in **2** is also based on O-H...O HBs of medium strength with O...O distances in the range 2.700 (3) - 2.981(3) Å. The water molecule of crystallization (O13w) plays a key role in the hydrogen bonding; it forms two HBs with two oxygen atoms, O8 and O11w, coordinated to Ce1, yielding a ring pattern  $R_2^2(6)$ ; moreover, O13w acts as an acceptor for a further two HBs, assuring connectivity between neighboring chains (Fig. 7). Among all of the HBs only one is intramolecular (*i.e.*, intrachain: O11...O5<sup>vii</sup>; vii: x, 5/2-y, z-1/2), the remaining ones being intermolecular. It is interesting that in **2** the nitrate group is involved in only one HB of the O-H...O type (O13w...O8<sup>xii</sup>; xii: x, y, 1+z) but it also acts as an acceptor in weaker HBs of the C-H...O type.

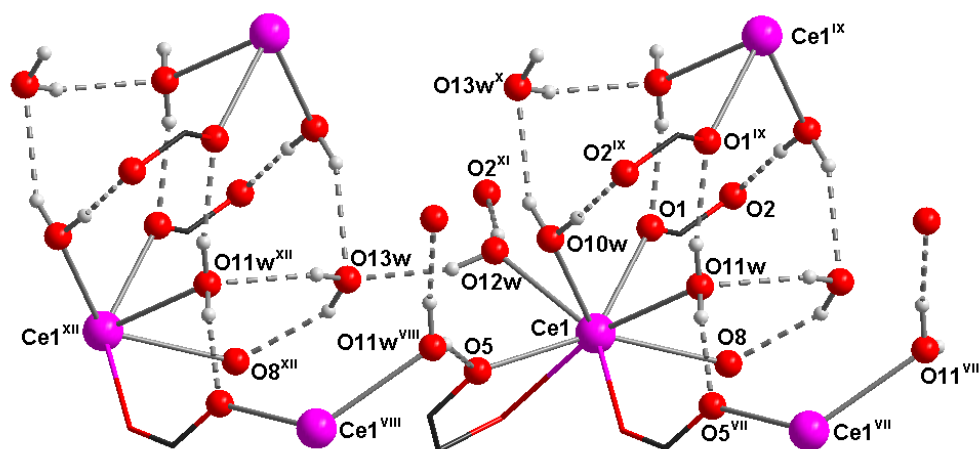


Fig. 7 Hydrogen bonding system in **2**. Symmetry codes: vii: x, 5/2-y, z-1/2; viii: x, 5/2-y, z+1/2; ix: -x, 2-y, -z; x: -x, 2-y, 1-z; xi: x, 3/2-y, z+1/2; xii: x, y, 1+z

<Table 3> Possible hydrogen bonds for **1** [ $\text{\AA}$ ,  $^\circ$ ]

D-H...A	d(D-H)	d(H...A)	d(D...A)	<(DHA)
O10w-H1w0...O5 <sup>ii</sup>	0.87(4)	2.01(5)	2.770(3)	145(4)
O10w-H2w0...O8 <sup>v</sup>	0.89(3)	2.00(3)	2.868(3)	166(3)
O11w-H1w1...O9 <sup>vi</sup>	0.72(4)	2.07(4)	2.751(3)	159(4)
O11w-H2w1...O1 <sup>i</sup>	0.88(4)	1.78(5)	2.625(3)	162(3)

Symmetry codes: i: 1-x, 1/2+y, 1/2-z ; ii: x, y-1, z ; v: 1-x, -y, -z ; vi: x, 1/2-y, 1/2+z

<Table 4> Possible hydrogen bonds for **2** [ $\text{\AA}$ ,  $^\circ$ ]

D-H...A	d(D-H)	d(H...A)	d(D...A)	<(DHA)
O10w-H1w0...O2 <sup>ix</sup>	0.85(4)	1.89(4)	2.732(5)	172(5)
O10w-H2w0...O13w <sup>x</sup>	0.85(5)	2.19(5)	2.977(5)	153(5)
O11w-H1w1...O1 <sup>ix</sup>	0.851(15)	1.93(3)	2.740(4)	159(5)
O11w-H2w1...O5 <sup>vii</sup>	0.85(2)	1.88(3)	2.700(4)	162(4)
O12w-H1w2...O2	0.851(9)	1.910(12)	2.753(5)	170(5)
O12w-H2w2...O13w	0.85(2)	1.91(2)	2.730(5)	160(5)
O13w-H1w3...O11w <sup>xii</sup>	0.85(4)	2.09(5)	2.841(5)	148(4)
O13w-H2w3...O8 <sup>xii</sup>	0.85(5)	2.01(4)	2.769(5)	147(5)

Symmetry codes: ix: -x, 2-y, -z ; x: -x, 2-y, 1-z ; vii: x, 5/2-y, z-1/2 ; xi: x, 3/2-y, z+1/2 ; xii: x, y, z+1

### 3.3 Magnetic properties of **1**

The temperature dependent magnetic data for the Ce(III) complex **1** are depicted in Fig. 8. As can be seen from the inset in this figure the effective magnetic moment gradually decreases from its room temperature value of  $\mu_{\text{eff}} = 3.27 \mu_{\text{B}}$  to the value of  $\mu_{\text{eff}} = 2.26 \mu_{\text{B}}$  at  $T = 1.8 \text{ K}$ . The analysis of the inverse susceptibility using the Curie-Weiss law performed above 50 K yielded  $\theta = -35.5(5) \text{ K}$  and this value may be influenced by both crystal field (CF) and intramolecular interactions present in the crystal. In order to clarify the dominant mechanism, in the first approximation, the properties of an isolated Ce(III) ion in the crystal lattice were considered.

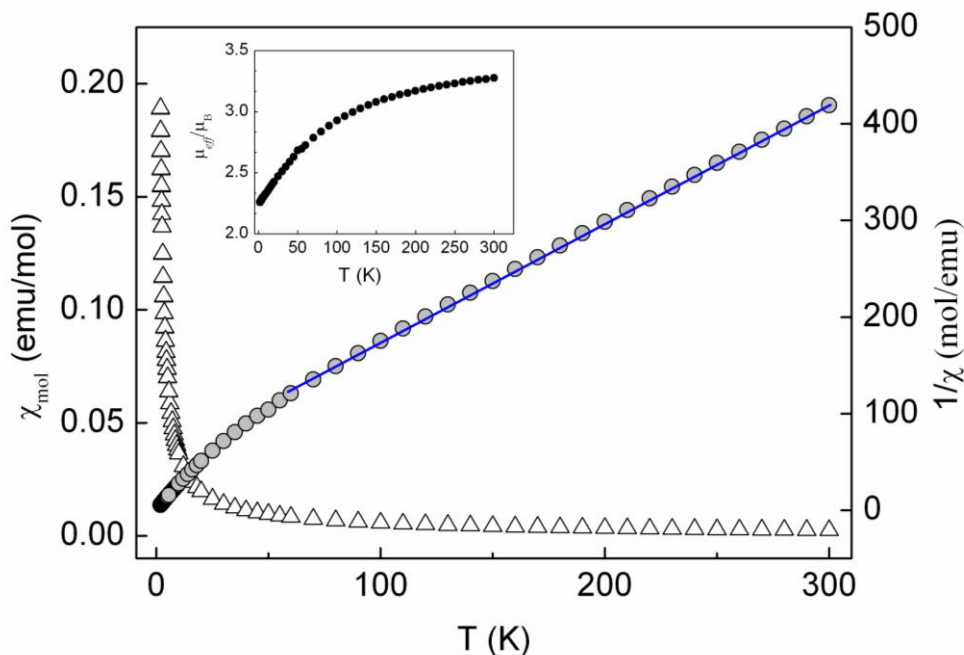


Fig. 8 Experimental magnetic curves for **1**: temperature dependence of the molar magnetic susceptibility (triangles); temperature dependence of the inverse magnetic susceptibility (grey circles); the result of the fit using Curie–Weiss law is denoted by the blue solid line. Inset: Temperature dependence of the effective magnetic moment (full circles).

The ground multiplet  $^2F_{5/2}$  of a Ce(III) ion is split by CF with symmetry lower than cubic into three Kramers doublets. Obviously, the energy differences within the doublets, which determine the temperatures at which the excited levels will become occupied, depend on the specific surroundings of the Ce(III) ions in **1**. In order to illustrate the effect, a comparison between the temperature dependence of the relative occupancy ratio  $n_2/n_1$  for two energy levels  $E_1$ ,  $E_2$  with energy difference  $\Delta_{12}$ , and the inverse susceptibility of **1**, was performed; the results are presented in Fig. 9. It should be noted, that for  $\Delta_{12}/k_B = 150$  K the excited level  $E_2$  starts to be thermally accessible nominally 30 K. This temperature is in very good agreement with

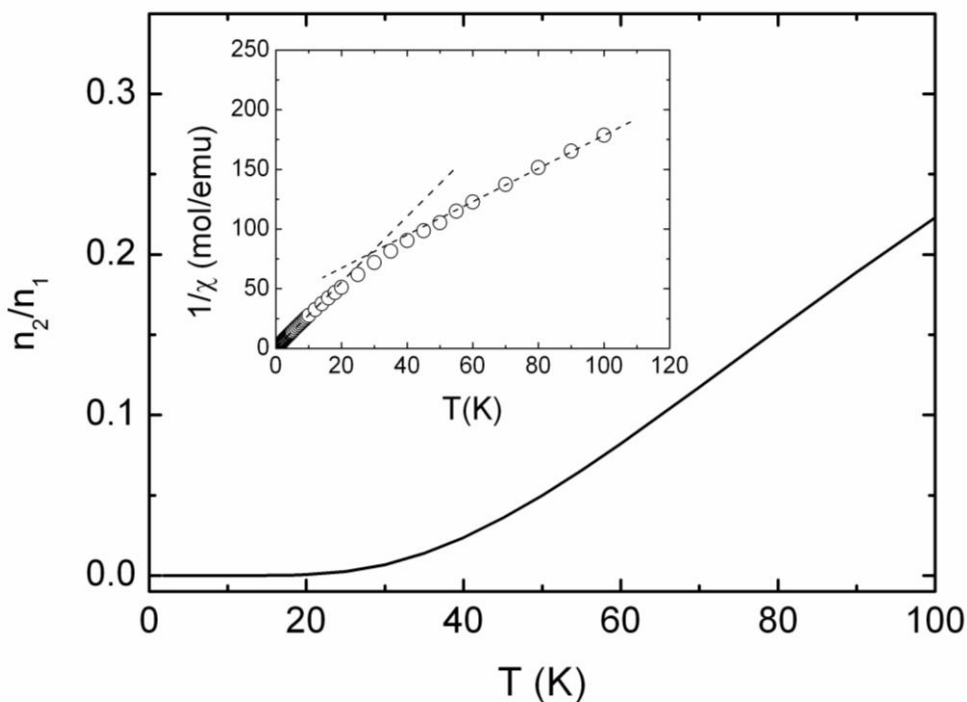


Fig. 9 Temperature dependence of the relative occupancy ratio for two energy levels with energy difference 150 K. Inset: temperature dependence of inverse susceptibility of **1**, the dashed lines are a guide for the eyes. See the text for a more detailed discussion.

the temperature at which the inverse susceptibility of **1** significantly deviates from the Curie–Weiss behavior found at temperatures above 50 K. The value obtained for  $\Delta_{12}$  seems to be plausible; a difference of the order of hundreds of Kelvins between excited levels was also found in other Ce(III) compounds [32]. Consequently, it may be suggested that CF effects represent the mechanism governing the behavior of the magnetic susceptibility, at least down to 30 K. In such a situation, the estimation of the exchange interaction among magnetic Ce(III) ions is less straightforward. Specific heat and magnetization studied at low enough temperatures ( $T \ll \Delta_{12}/k_B$ ) would represent informative quantities for establishing magnetic dimensionality and determining the magnitude of magnetic interactions in this system.

#### 4. Summary

Using hydrothermal conditions two new heteroleptic Ce(III) complexes  $[\text{Ce}(\text{PDOA})(\text{NO}_3)(\text{H}_2\text{O})_2]_n$  (**1**) and  $\{[\text{Ce}(\text{PDOA})(\text{NO}_3)(\text{H}_2\text{O})_3] \cdot \text{H}_2\text{O}\}_n$  (**2**) were isolated and characterized. While the formation of **1** was straightforward, **2** formed only as a byproduct in the presence of phen. The results of X-ray structure analyses revealed that PDOA acts as a hexadentate ligand in **1** and is pentadentate in **2**. As a consequence, in **1** each Ce(III) atom is connected with four neighbors and a ribbon-like arrangement of Ce(III) atoms can be observed, while in **2** each Ce(III) atom is connected only with two other Ce(III) atoms and a zig-zag chain-like arrangement is formed; both 1d structural motifs are new among the o-phenylenedioxydiacetato complexes of lanthanides. A rich system of hydrogen bonds

1 stabilizes both crystal structures. The magnetic properties of **1** above 50 K can be described  
2 using Curie-Weiss behavior with  $\theta = -35.5$  K.  
3

#### 4 **Appendix A. Supplementary data**

5 CCDC 1029869 and CCDC 1029871 contain the supplementary crystallographic data for  
6 complexes **1** and **2**, respectively. These data can be obtained free of charge via  
7 <http://www.ccdc.cam.ac.uk/conts/retrieving.html>, or from the Cambridge Crystallographic  
8 Data Centre, 12 Union Road, Cambridge CB2 1EZ, UK; fax: (+44) 1223-336-033; or e-mail:  
9 [deposit@ccdc.cam.ac.uk](mailto:deposit@ccdc.cam.ac.uk).  
10  
11  
12  
13

#### 14 **Acknowledgements**

15 This work was supported by the Slovak grants VEGA (grant No. 1/0075/13), APVV-0132-11  
16 and APVV-0014-11. Funding from the Ministry of Science and Innovation (Spain) under  
17 grants MAT2011-27233-C02-1 and CONSOLIDER 25200 and from the Diputación General  
18 de Aragón is gratefully acknowledged. This publication is the result of the Project  
19 implementation: KVARC (ITMS: 26110230084), supported by the Research & Development  
20 Operational Program funded by the ESF.  
21  
22  
23  
24  
25  
26  
27  
28  
29  
30  
31  
32  
33  
34  
35  
36  
37  
38  
39  
40  
41  
42  
43  
44  
45  
46  
47  
48  
49  
50  
51  
52  
53  
54  
55  
56  
57  
58  
59  
60  
61  
62  
63  
64  
65

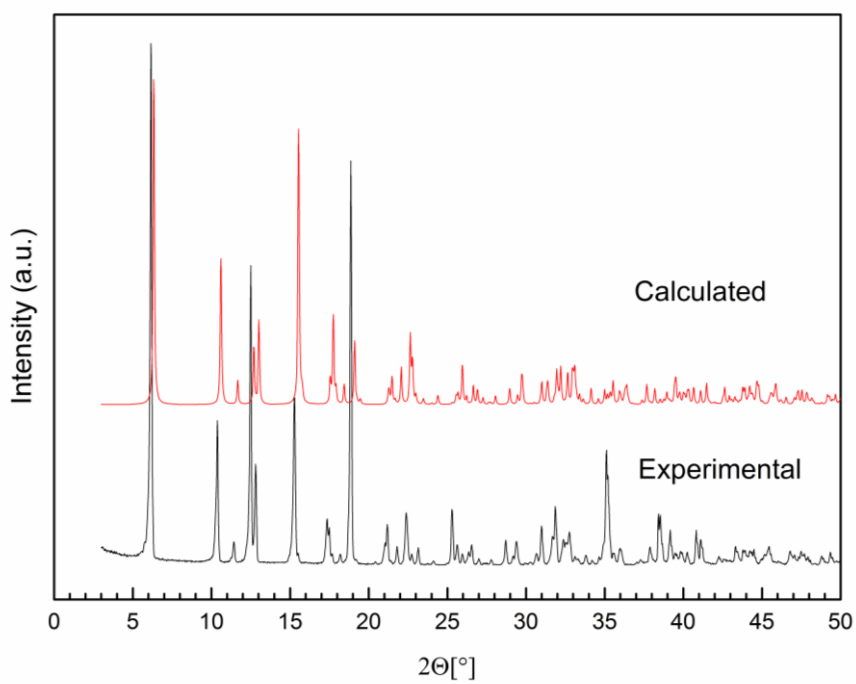


## References

- [1] C. Qin, X.L. Wang, E.B. Wang, L. Xu, *Inorg. Chem. Com.* 8 (2005) 669-672.
- [2] S.V. Eliseeva, J.-C.G. Buezli, *Chem. Soc. Rev.* 39 (2010) 189-227.
- [3] Y.J. Cui, Y.F. Yue, G.D. Qian, B.L. Chen, *Chem. Rev.* 112 (2012) 1126-1162.
- [4] J. Wang, W.P. Wu, L. Lu, L.K. Zou, B. Xie, *J. Chem. Res.* 37 (2013) 73-76.
- [5] J. J. Baldovi, S. Cardona-Serra, J. M. Clemente-Juan, *Inorg. Chem.* 51 (2012) 12565-12574.
- [6] F. Caille, C.S. Bonnet, F. Buron, S. Villette, L. Helm, S. Petoud, F. Suzenet, E. Toth, *Inorg. Chem.*, 51 (2012) 2522-2532.
- [7] J. Vanek, P. Lubal., P. Hermann, P. Anzenbacher, *J. Fluorescence* 23 (2013) 57-69.
- [8] R. Mohammadinasab, M. Tabatabaee, B.-M. Kukovec, H. Aghaie, *Inorg. Chim. Acta* 405 (2013) 368-373.
- [9] D.Y. Ma, L. Qin, H.F. Guo, J.X. Lin, H.C. Wei, *Synth. Metals* 175 (2013) 30-35.
- [10] C.A.F. de Oliveira, F.F. da Silva, I. Malvestiti, V.R.D. Malta, J.D.L. Dutra, N.B. da Costa, R.O. Freire, S. Alves, *J. Mol. Struct.* 1041 (2013) 61-67.
- [11] H.-H. Song, Y.-J. Li, Y. Song, Z.-G. Han, F. Yang, *J. Sol. State Chem.* 181 (2008) 1017-1024.
- [12] C.-G. Wang, Y.-H. Xing, Z.-P. Li, J. Li, X.-Q. Zeng, M.-F. Ge, S.-Y. Niu, *J. Mol. Struct.* 921 (2009) 126-131.
- [13] P. Gawryszewska, Z. Ciunik, *J. Photochem. Photobiol.A – Chem.* 202 (2009) 1-9.
- [14] X. Li, X.-S. Wu, H.-L. Sun, L.-J. Xu, G.-F. Zi, *Inorg. Chim. Acta* 362 (2009) 3837 - 3841.
- [15] Y. Jiang, X.-S. Wu, X. Li, J.-H. Song, Y.-Q. Zou, *J. Coord. Chem.* 63 (2010) 36-45.
- [16] X. Li, C.-Y. Wang, X.-J. Zheng, Y.-Q. Zou, *J. Coord. Chem.* 61 (2008) 1127-1136.
- [17] F.H. Allen, *Acta Cryst.*, B58 (2002) 380-388.
- [18] T. Behrsing, G.B. Deacon, P.C. Junk, B.W. Skelton, A.N. Sobolev, A.H. White, *Z. Anorg. Allg. Chem.* 639 (2013) 41-48.
- [19] M. Stolárová, J. Černák, M. Tomás, I. Ara, L.R. Falvello, R. Boča, J. Titiš, *J. Coord. Chem.* 67 (2014) 1046-1060.
- [20] C.F. Macrae, I.J. Bruno, J.A. Chisholm, P.R. Edgington, P. McCabe, E. Pidcock, L. Rodriguez-Monge, R. Taylor, J. van de Streek and P.A. Wood. *J. Appl. Cryst.* 41 (2008) 466-470.
- [21] R.L. Carlin, & A.J. van Duyneveldt, *Magnetic Properties of Transition Metal Compounds.* Springer, New York, NY, USA, 1977.
- [22] SADABS-2008/1: Area-Detector Absorption Correction. Bruker-AXS (2008).
- [23] A. Altomare, G. Cascarano, C. Giacovazzo, A. Gualardi, *J. Appl. Cryst.*, 26, 343 (1993).
- [24] G.M. Sheldrick. *Acta Crystallogr.* A64 (2008) 112.
- [25] K. Brandenburg, H. Putz. *Crystal Impact Diamond, Crystal and Molecular Structure Visualization,* GbR, Postfach 1251, D-53002 Bonn, Germany (2008).

- 1  
2  
3  
4  
5  
6  
7  
8  
9  
10  
11  
12  
13  
14  
15  
16  
17  
18  
19  
20  
21  
22  
23  
24  
25  
26  
27  
28  
29  
30  
31  
32  
33  
34  
35  
36  
37  
38  
39  
40  
41  
42  
43  
44  
45  
46  
47  
48  
49  
50  
51  
52  
53  
54  
55  
56  
57  
58  
59  
60  
61  
62  
63  
64  
65
- [26] K. Nakamoto, *Infrared and Raman Spectra of Inorganic and Coordination Compounds, Part B: Applications in Coordination, Organometallic, and Bioinorganic Chemistry*, Wiley, New York, 1997.
- [27] P. Gawryszewska, Z. Ciunik, D. Kulesza, *J. Mol. Struct.* 988 (2011) 59.
- [28] M. Llunell, D. Casanova, J. Cirera, P. Alemany, S. Alvarez, *SHAPE - Program for the Stereochemical Analysis of Molecular Fragments by Means of Continuous Shape Measures and Associated Tools, Version 2.1*, University of Barcelona, Spain, March 2013.
- [29] G. Smith, R.C. Bott, D.S. Sagatys, C.H.L. Kennard, *Polyhedron* 10 (1991) 1565-1568.
- [30] X.-F Li, Z.-B. Han, *Acta Crystallogr., Sect. E*, 62 (2006) m2024.
- [31] H.-M. Guo, *Acta Cryst.* E66 (2010) m1602.
- [32] K. Yutani, Y. Muro, J. Kajino, T.J. Sato, and T. Takabatake, *J. Physics: Conference Series* 391 (2012) 012070-4.

Supplementary material:



<Fig. S1> Experimental and calculated powder X-ray diffraction pattern for **1**.

CIF (\*if crystal structure is described)

[Click here to download CIF \(\\*if crystal structure is described\): ial272a.cif](#)

CIF (\*if crystal structure is described)

[Click here to download CIF \(\\*if crystal structure is described\): ial274b.cif](#)

CheckCIF (\*if crystal structure is described)

[Click here to download CheckCIF \(\\*if crystal structure is described\): checkcif-ial272a.pdf](#)

CheckCIF (\*if crystal structure is described)

[Click here to download CheckCIF \(\\*if crystal structure is described\): checkcif-ial274b.pdf](#)